Contract N00014-76-C-0495

LEVEL II

12

FUNDAMENTAL INVESTIGATION OF PITTING CORROSION IN STRUCTURAL METALS

THEODORE R. BECK

ELECTROCHEMICAL TECHNOLOGY CORP.
3935 LEARY WAY N.W.
SEATTLE, WA 98107
(206) 632-5965

FINAL REPORT FOR PERIOD JULY 1975 - JUNE 1981

Prepared for

OFFICE OF NAVAL RESEARCH
800 North Quincy Street
Arlington, VA 22217

July 1981

Unclassified

SECURITY CLASSIFICATION OF THIS PAGE (When Data Entered)

REPORT DOCUMENTATION PAGE	READ INSTRUCTIONS BEFORE COMPLETING FORM
1. REPORT NUMBER	2. GOVT ACCESSION NO. AD-A102 338 / 3. RECIPIENT'S CATALOG NUMBER
4. TITLE (and Subtitle) Fundamental Investigation of Pitting Corrosion in Structural Metals	5. TYPE OF REPORT & PERIOD COVERED Final Report Jul 1975 — Jun 1981
	6. PERFORMING ORG. REPORT NUMBER
7. AUTHOR(s) Theodore R. Beck	8. CONTRACT OR GRANT NUMBER(s) N00014-76-C-0495
9. PERFORMING ORGANIZATION NAME AND ADDRESS Electrochemical Technology Corp. 3935 Leary Way N.W. Seattle, WA 98107	10. PROGRAM ELEMENT, PROJECT, TASK AREA & WORK UNIT NUMBERS
11. CONTROLLING OFFICE NAME AND ADDRESS	12. REPORT DATE Jul 1981
	13. NUMBER OF PAGES 20
14. MONITORING AGENCY NAME & ADDRESS (if different from Controlling Office) Office of Naval Research Materials Science Division Arlington, VA 22217	15. SECURITY CLASS. (of this report) Unclassified
	15a. DECLASSIFICATION DOWNGRADING SCHEDULE

16. DISTRIBUTION STATEMENT (of this Report)

17. DISTRIBUTION STATEMENT (of the abstract entered in Block 20, if different from Report)

Reproduction in whole or part is permitted for any purpose of the United States Government. Distribution is unlimited.

18. SUPPLEMENTARY NOTES

19. KEY WORDS (Continue on reverse side if necessary and identify by block number)

Corrosion, pitting, iron, aluminum, magnesium, titanium, stainless steel, mass transport, salt film.

20. ABSTRACT (Continue on reverse side if necessary and identify by block number)

This report gives a summary of the main electrochemical features of pitting corrosion of iron, aluminum, magnesium, titanium, and stainless steel in halide solutions. Ohmic and mass transport limited corrosion regions and effect of hydrodynamic flow are described. Barrier films of metal halide salt are formed on the metal surface for these metals in the mass transport limited region. The electrical properties of these salt films were determined. A mechanism is proposed for the protection from pitting of stainless steels by flowing seawater.

DD FORM 1 JAN 73 1473 EDITION OF 1 NOV 65 IS OBSOLETE

Unclassified

SECURITY CLASSIFICATION OF THIS PAGE (When Data Entered)

INTRODUCTION

The objective of the contract work was to develop a more quantitative electrochemical understanding of the pitting corrosion phenomona for structural metals of interest to the Navy. The metals studied included titanium, aluminum, magnesium, iron, and 304 stainless steel. These metals are normally protected by a passive oxide film, but under certain circumstances, the oxide is breached in localized regions and pitting corrosion occurs.

Pitting of passive metals is a very complex phenomenon, particularly under natural conditions. Fig. 1 illustrates some of the complexities. The pit occurs at a breach in the protective passive oxide film. The film may remain in position covering the pit, or it may be removed. The pitting reaction proceeds because a simultaneous reduction, usually that of oxygen from the atmosphere, occurs. The rate of oxygen reduction may be mass transport limited, thus limiting the total pitting current. Current is carried in solution by ionic species, and there may be a significant ohmic drop in solution. The pits occur randomly on the surface, being nucleated at defects in the oxide film. The pits may be of various ages and sizes. They may not all be active at once. Their geometry is approximately hemispherical, but it is variable. Because of all of these complexities, it is difficult to conduct definitive experiments regarding events within the pits under the conditions illustrated in Fig. 1.

The approach used in the present work was to idealize a pit to a shape and conditions that can be more precisely defined. After the events within the pit are quantitatively understood, the component parts of the whole pitting system can be put together again with appropriate experimental or modeling techniques.

The pit geometry used was the "shielded electrode" of W. J. Muller shown in Fig. 2. A rod of the metal under investigation is cast in epoxy resin, and only one end is corroded. At a depth equal to or greater than the "pit" diameter or width, the current density becomes extremely uniform on the bottom of the pit. Ionic conduction and mass transport processes within the "pit" become one-dimensional and amenable to more rigorous analysis than for natural, approximately-hemispherical, pits.

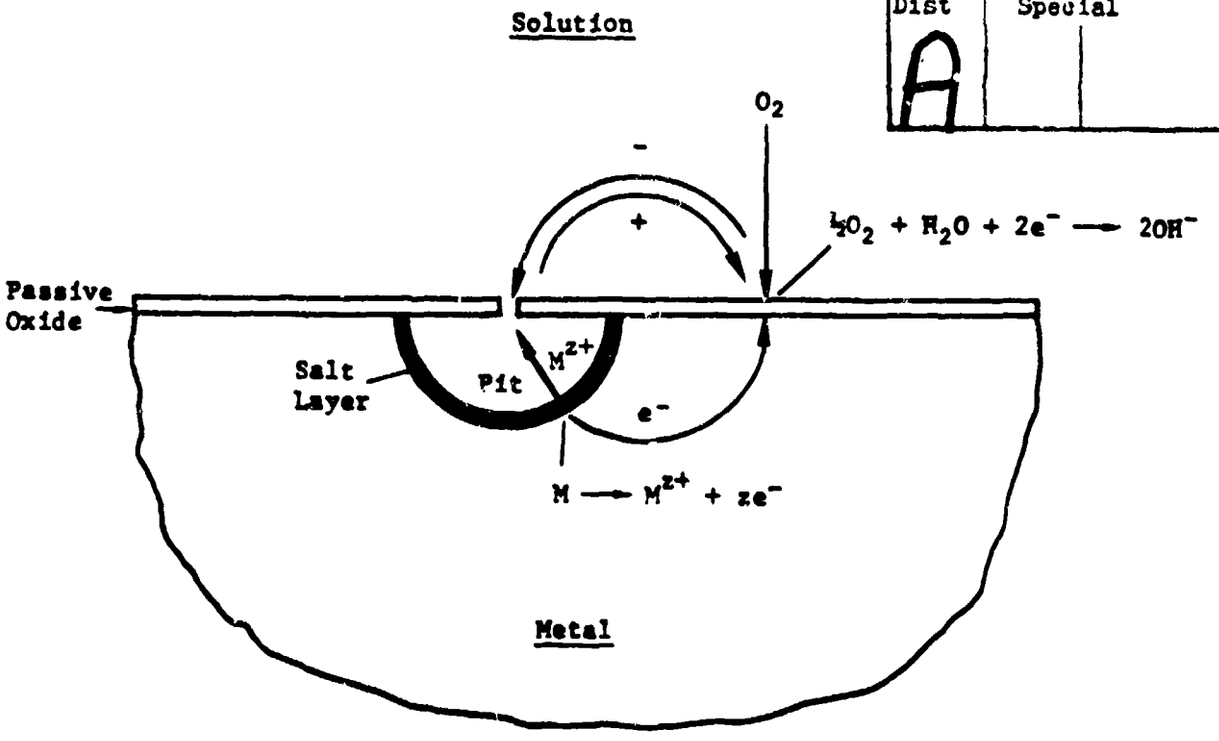

Fig. 1. Pit in passive metal driven by oxygen reduction on adjacent passive surface

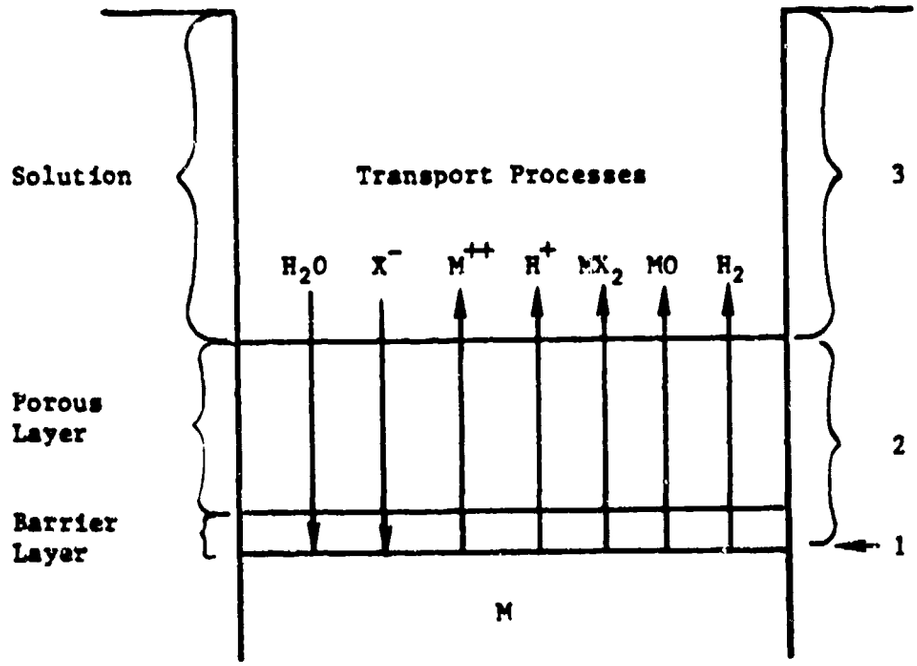

Reactions at 1

$$M \longrightarrow M^{++} + 2e$$
$$M + H_2O \longrightarrow MO + 2H^+ + 2e$$
$$2H^+ + 2e \longrightarrow H_2$$

Reactions in 2 and 3

$$MX_2 \rightleftharpoons M^{++} + 2X^-$$
$$M^{++} + H_2O \longrightarrow MO + 2H^+$$

Fig. 2. One-dimensional pit, reactions and transport processes (divalent metal ion used for illustration).

Potential or current to an artificial pit can be controlled with a potentiostat.

Even the idealized one-dimensional pit has complex electrochemistry. Layers of halide or oxyhalide salts form on the bottom of the pit. There is an inner barrier layer with ohmic or high-field conducting properties and usually an outer variable porous layer, observable under a microscope. The pitting current density is limited by the rate that the salt can be transported out of the pit.

Three types of reactions may occur at the metal-to-barrier-layer interface as illustrated in Fig. 2. First, the metal reacts electrochemically to form its ion. The halide salt in the barrier layer forms either by transport of halide ion to the metal surface or by transport of the metal ion through the barrier layer to the outer barrier layer interface where it meets halide ion, or both. The second type reaction is formation of oxide at the metal surface by electrochemical reaction with water which has diffused through the barrier layer. The third type reaction is reduction of hydrogen ion or water to form hydrogen gas. Hydrogen ions are available from the oxide formation reaction. The potential of the metal-to-barrier-layer interface is negative enough for titanium, aluminum, and magnesium to produce significant amounts of hydrogen. The hydrogen gas generated during pitting of aluminum and magnesium is sufficient to produce convection that affects transport processes in the pit.

In the porous layer and in the solution in the pit further reaction can occur. The salt can dissolve and ionize. The salt or its cation can hydrolyze to form hydroxide or oxide. Formation of oxide at any place in the pit gives acidification which can result in dissolution of the oxide. Coupling this set of reactions to the transport of various species, H_2O, halide ion, metal ion, hydrogen ion, metal salt, oxide, and hydrogen gives a complex system for modeling. It is not surprising that the mechanism of pitting is imperfectly understood.

A variety of techniques was employed to study the one-dimensional pitting system illustrated in Fig. 3. Potentiodynamic current-voltage curves provided information on the ohmic-limited and mass transport

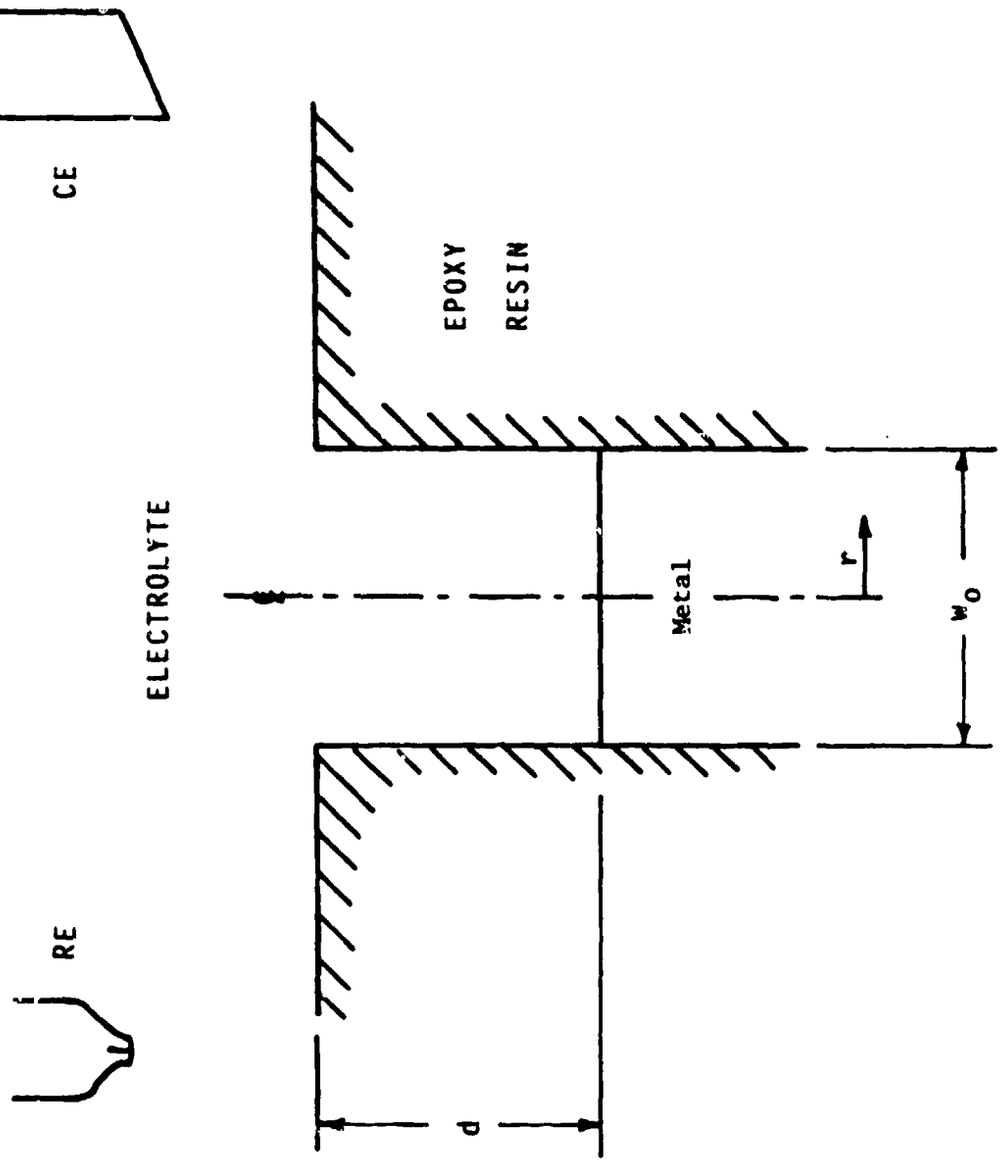

Fig. 3 Experimental arrangement for one-dimensional pitting experiments (w_o = 0.16 cm)

limited regimes. Electrolyte flow past the mouth of the pits with the flow cell illustrated in Fig. 4 gave quantitative mass transport data. Potentiostatic current-time data under stagnant electrolyte conditions gave further quantitative correlations of unsteady-state mass transport. On a shorter time scale, current transients from step potential experiments provided information on the electrical properties of the barrier salt film. Open-circuit potential decay experiments provided further data on salt-film electrical properties. Volumetric rates of hydrogen evolution were also measured, as well as apparent valence of metal dissolution. In order to study individual small pits in stainless steel, the artificial pit illustrated in Fig. 5 was used.

SUMMARY

A brief summary of the results for the various metals is presented here. More detailed data are given in the papers published and in progress.

Potentiodynamic Curves, Effect of Hydrodynamic Velocity

A typical potentiodynamic curve is shown in Fig. 6 (Tech. Rept. 5). This curve is for magnesium, but similar shapes are found for other metals. In the ascending, approximately-linear region up to ϕ_p, i_p, the current density is limited by the ohmic resistance in solution between the working electrode surface and the reference electrode. Iron has an etched surface in this region, whereas titanium, aluminum, and magnesium develop microtunneling. At the peak, ϕ_p, i_p, salt precipitation occurs and the current density decreases to a low value, determined by the mass transport rate of the corroding metal ion out of the pit. In this region, the metal surface is electropolished. On the negative potential sweep, the current density remains at the mass transport limited rate to a lower potential because there is less agitation by coevolved hydrogen bubbles. The effect of electrolyte velocity past the mouth of the pit in the flow cell is shown in Fig. 7. Results for iron are given in Technical Report No. 1.

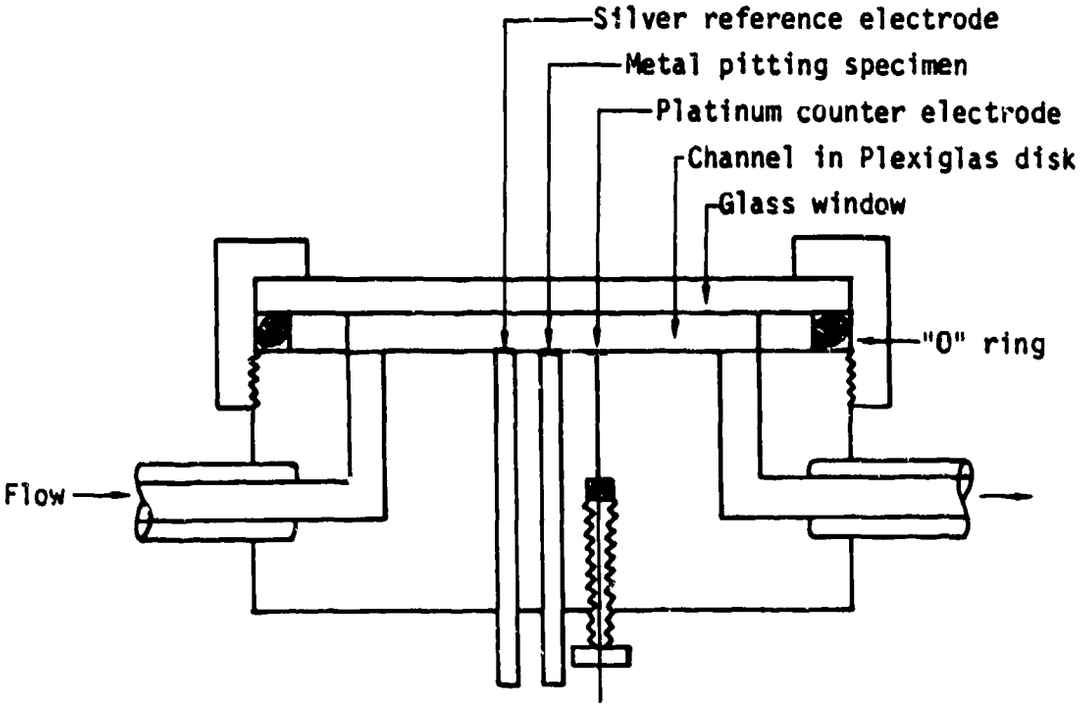

Fig. 4 Cutaway section of flow channel cell used to determine hydrodynamic effects on current density in small pits.

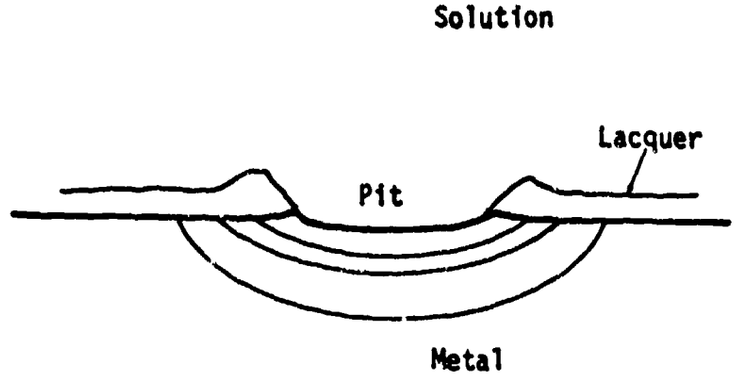

Fig. 5 Single artificial pit in hole in lacquer layer showing approximate corrosion profiles. (Diameter of pit approximately 0.0070 cm.)

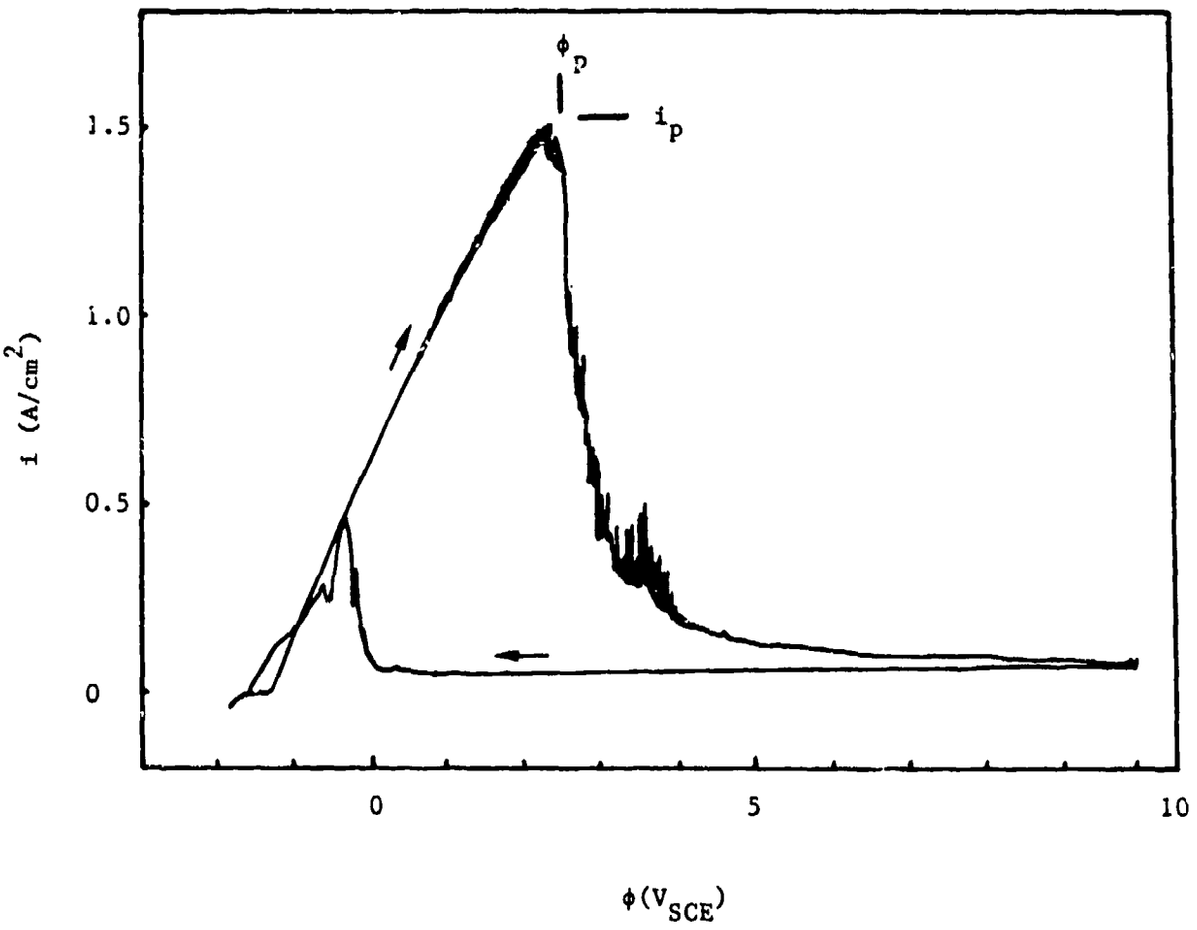

Fig. 6 Potentiodynamic polarization curve for magnesium in 0.94 M $MgCl_2$; depth = 2 mm; sweep rate = V/min.

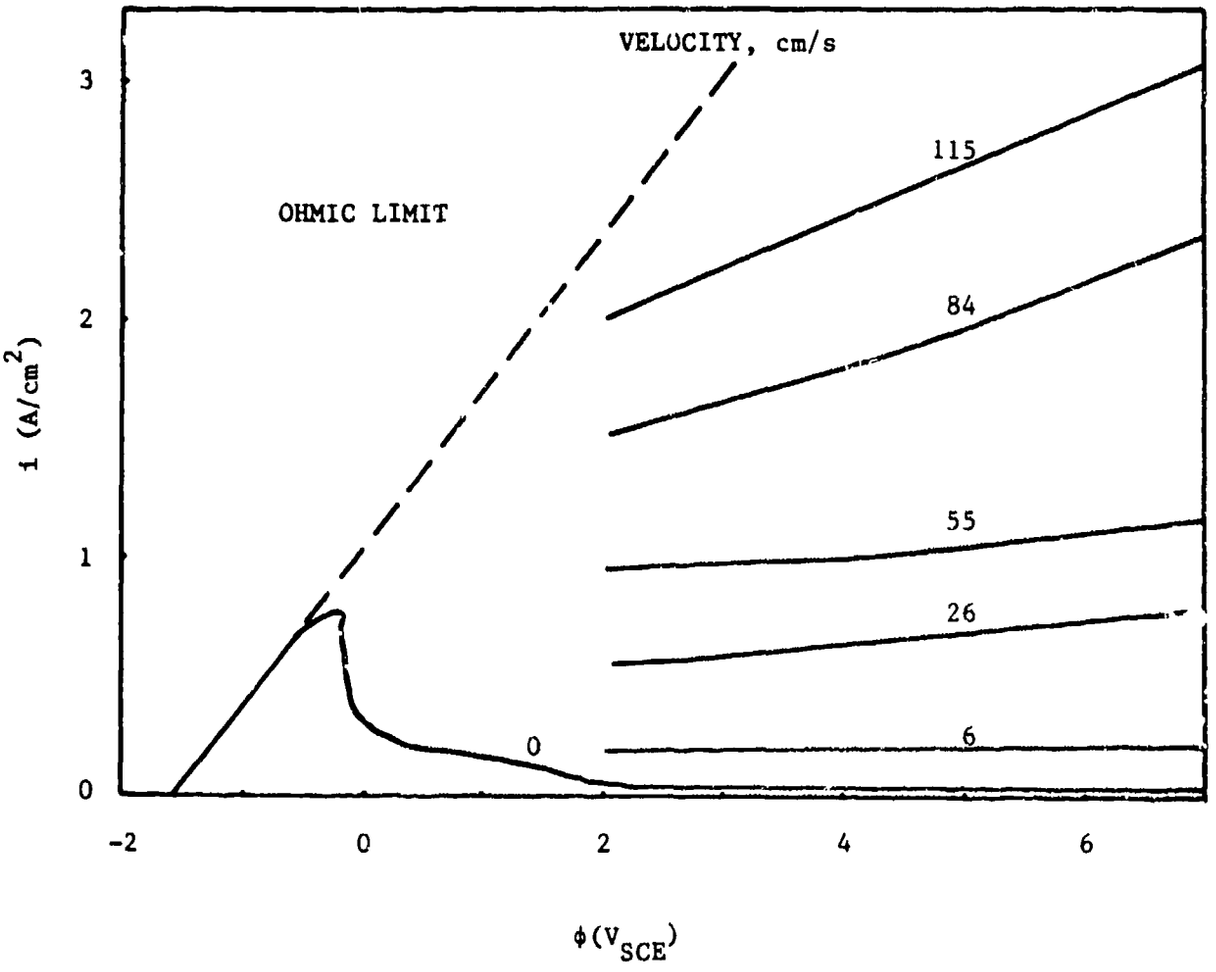

Fig. 7 Effect of electrolyte velocity on current density in mass transport limited region in 4.7 M $MgCl_2$; depth = 1.5 mm.

Hydrogen Evolution and Apparent Valence

Rate of hydrogen evolution accompanying pitting was determined for titanium, aluminum, and magnesium. Data for magnesium are given in Fig. 8 (Tech. Rept. 5). The hydrogen rate was measured with a gas microburette inverted over the mouth of the pit. The equivalent hydrogen current density was calculated from Faraday's law. The ratio of the hydrogen current density to the anodic current density is 0.3 in the ohmically limited region, and 0.001 to 0.02 in the mass transport limited region. The dashed curve in Fig. 8 is

$$\frac{i_{H_2}}{i_a} = \frac{0.0205}{(\phi + 1.9)} \qquad (1)$$

Such a relationship is consistent with a limiting diffusion rate of water through a salt film with thickness proportional to potential above that for formation of $MgCl_2$ (-1.9 V_{SCE}). The apparent valence of dissolution of magnesium in the ohmic region is about 1.4, and in the mass transport region 2.0. These values are consistent with the rate of hydrogen evolution. Titanium and aluminum also had greater hydrogen rates in the ohmic region as compared to the mass transport region.

Current Density-Time Curves

Typical current density-time curves after application of a step potential are shown in Fig. 9 (Tech. Rept. 2). These curves are for pure iron in 6 N HCl; similar shapes are found for the other metals. The initial current density at the left is ohmically limited. At the knees of the curves, denoted by τ^*, green salt crystals ($FeCl_2$) could be seen growing on the metal surface. The dashed line, a, was calculated from Sand's equation

$$i = 1/2\ zFC_s\sqrt{\frac{\pi D}{\tau_s}} \qquad (2)$$

which gives a relation between the initial current density and the time to reach saturation of $FeCl_2$ on the iron surface. The actual time exceeded

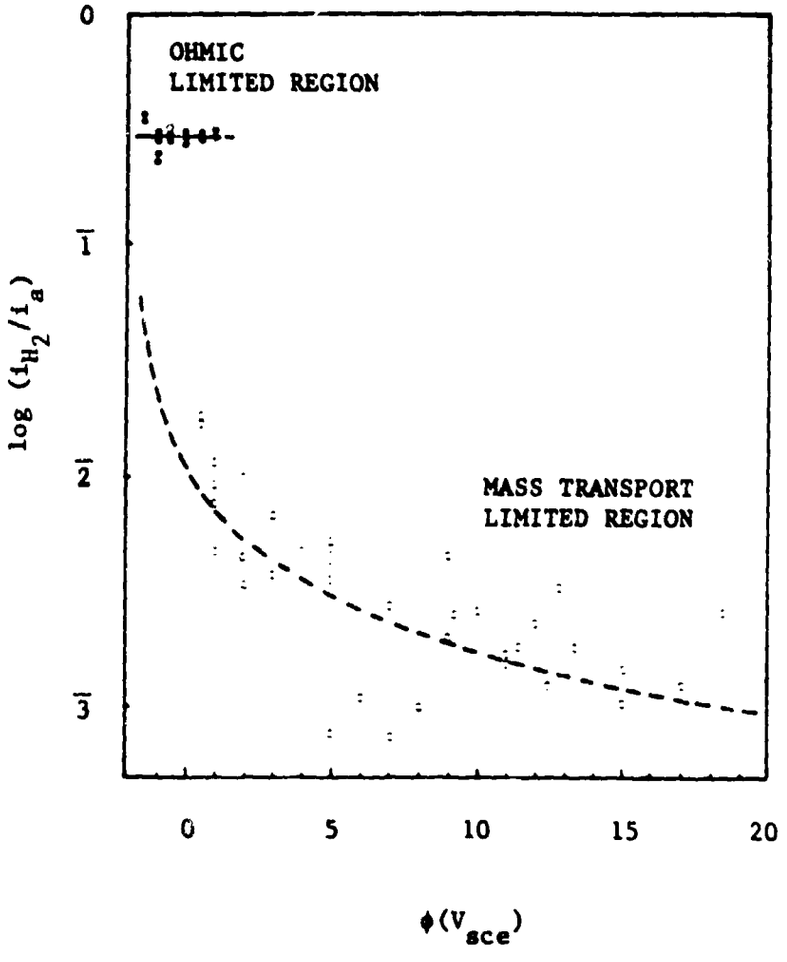

Fig. 8 Ratio of hydrogen current density to anodic current density in ohmic limited and mass transport limited regions for 0.94 M $MgCl_2$.

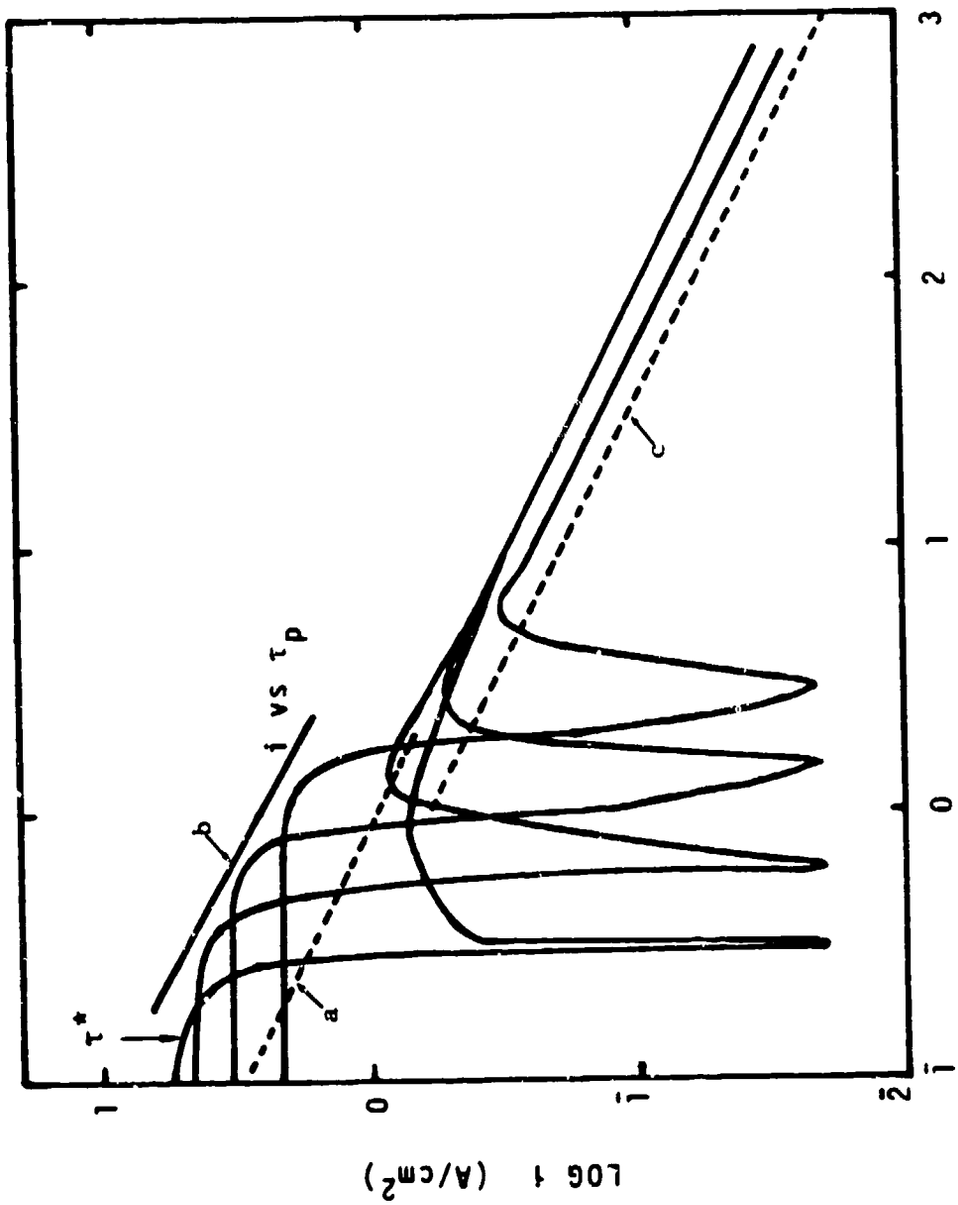

Fig. 9 Current density transients for step potentials with pure iron in 6N HCl; a = Sand's equation, b = i vs τ_p, c = equation 3.

this value, indicating supersaturation. The overshoot in current density decay is due to the precipitated salt layer. At the minimum in the current, the precipitated salt crystals dissolved and a transparent salt layer remained. The final decay in current density can be attributed to growth of the diffusion layer thickness to fill the pit. The diffusion limiting current density can be described by

$$i_L = zFC_s\sqrt{\frac{D}{\pi t}} \tag{3}$$

Eq. 3 is plotted as line c in Fig. 9. The actual data are higher than line c, probably due to contribution by electrolytic migration of Fe^{++}. At a time of about 10^3 s, the current density becomes constant for steady state diffusion out of a 0.1 cm deep pit.

Fast Electrical Transients

Rapid transient response of current density to step changes in potential under mass transport limiting conditions can be used to determine the barrier salt film properties. At the mass transport limit, most of the potential trop in the pit is across the salt film. The initial peak current densities are a function of the initial potential, ϕ_1, which determines the initial thickness, t_1. Ohmic and high-field conduction give the following equations respectively.

$$i_p = \frac{\kappa(\phi_1 - \phi_e + \Delta\phi)}{t_1} \tag{4}$$

and

$$i_p = i_o \exp\left[\frac{(\beta_1 - \phi_e + \Delta\phi)}{t_1}\right] \tag{5}$$

It turns out that magnesium and titanium halides have high field conduction, and iron and aluminum halides are ohmic. Data for magnesium are shown in Fig. 10 (Tech. Rept. 5). Values of t_1/β are found to be linear with potential in agreement with the barrier layer thickness being proportional to potential and a constant value of β. At high current densities, there appears to be an additional series ohmic resistance. Experimental results

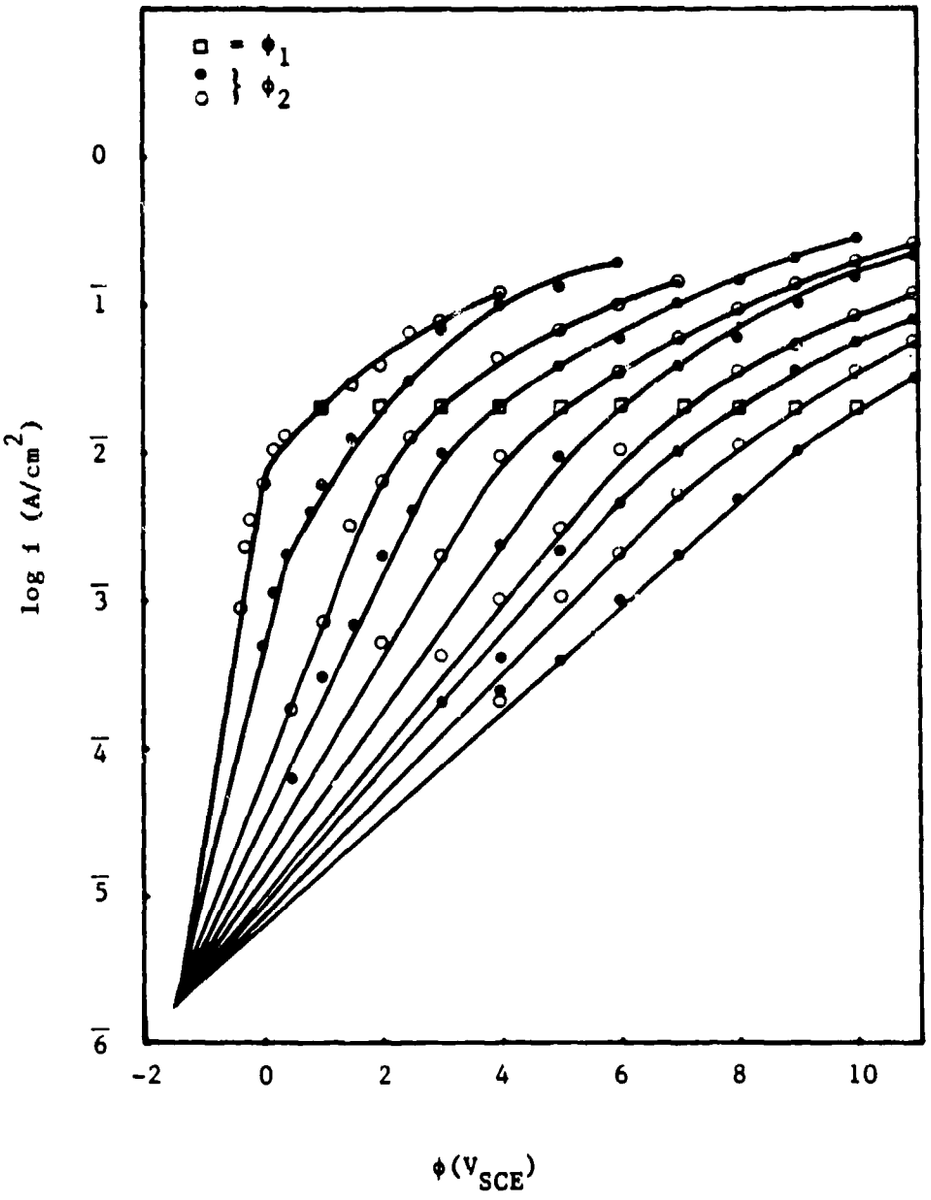

Fig. 10 Plots of initial current densities after step potential to ϕ_2 from ϕ_1 in 4.2 M $MgCl_2$.

indicate that this ohmic resistance may be due to the outer porous salt layer.

Open-circuit potential transients were also used to determine the barrier film properties and gave consistant results to the step potential experiments.

Velocity Effects with Stainless Steel

It has long been known that stainless steels are subject to pitting attack in stagnant seawater, and seawater velocities greater than 5 ft/s are recommended to avoid pitting. The mechanism of protection by flowing seawater was not previouly established, however. Results from the present work of flow experiments with small pits and analysis of effects of the hydrodynamic conditions on mass transport of corrosion products showed that flow of 5 ft/s limits pits to micrometer size. Even though pits may nucleate, they are extinguished by fluid flow when they reach a certain size.

The relation of critical velocity for extinguishing corrosion versus pit radius is shown in Fig. 11(Tech. Rept. 3). Two curves are shown in Fig. 11, one for 1 N NaCl used in the experiments, and one calculated for seawater (0.6 N NaCl). Pitting is allowed at velocities below the curves and not allowed above the curves. For example, for a velocity of 5 ft/s (152 cm/s), the maximum pit radius allowed is about 2 μm, invisible to the naked eye.

Many experiments were conducted to test the relationship in Fig. 11. Pits established on a flat surface of 304 stainless steel under stagnant conditions and allowed to grow to a size visible under a binocular microscope at 60X were completely extinguished by subsequent flow of electrolyte. The experiments were not as quantitative as desired though, because a distribution of pit sizes was obtained. Two methods were used to obtain single pits of controlled size. One was to coat a stainless steel specimen with a lacquer and punch a hole in the lacquer with a pin (Fig. 5). The other method was to make an artificial pit by corroding the ends of various-diameter stainless steel wires embedded in epoxy resin

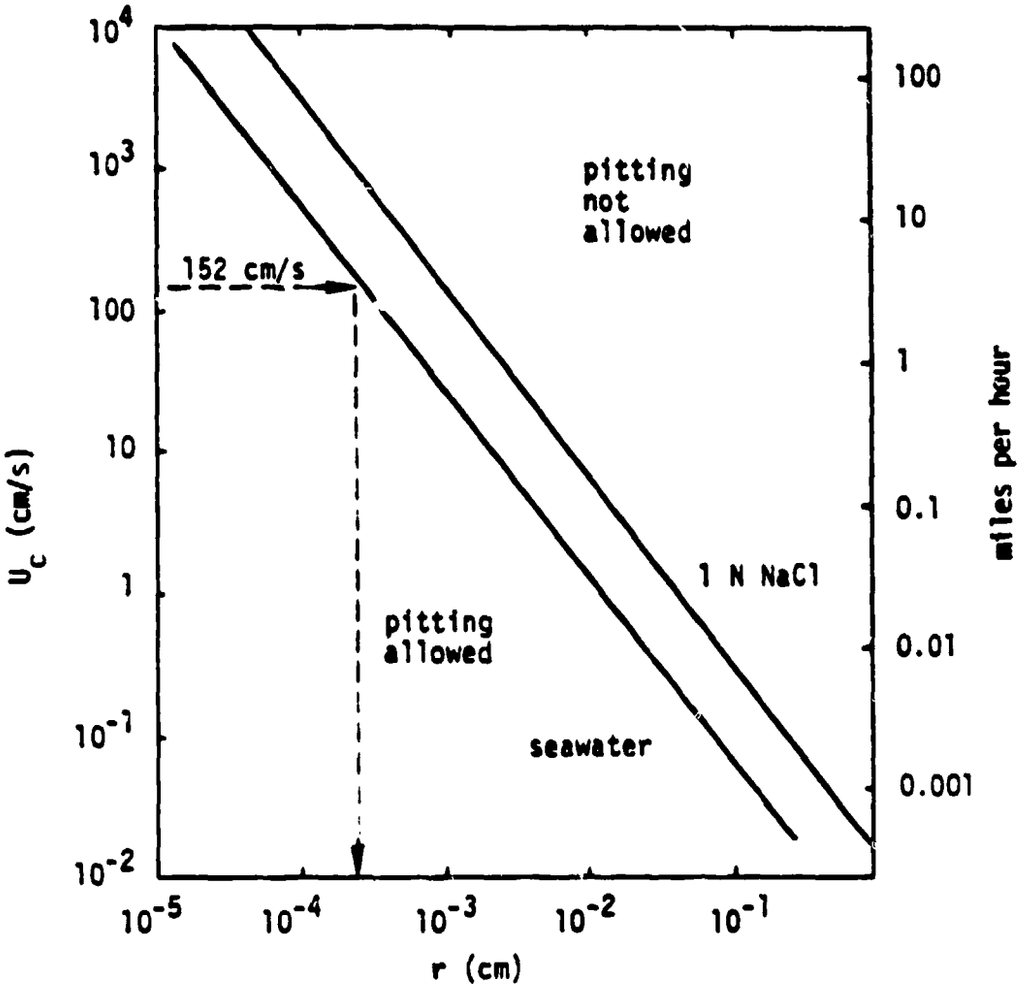

Fig. 11 Critical velocity for pitting of passivating metal as a function of pit radius.

(Fig. 3). In both of these cases of artificial pits, flow caused the pitting current to decrease at the appropriate velocity according to Fig. 11; but the current did not go to zero. It was found that crevice corrosion continued between the stainless steel and the lacquer or the epoxy resin.

Formation of Salt Films in Small Pits

A mass transport analysis of small pits showed that at moderate salt concentrations, such as in seawater, the initial corrosion current densities may be very large and a salt of the corroding metal is likely to form on the metal surface (Tech. Rept. 4). Observations of pitting under a microscope indicated that a salt film was present in the pits in stainless steel.

INDEX OF TECHNICAL REPORTS (submitted with DD 1473)

1. Effects of Hydrodynamics on Pitting, April, 1977 (Publication No. 1).
2. Formation of Salt Films During Passivation of Iron, December, 1978 (Publication No. 6).
3. Experimental Observations and Analysis of Hydrodynamic Effects on Growth of Small Pits, June, 1979 (Publication No. 4).
4. Occurance of Salt Films During Initiation and Growth of Corrosion Pits, March, 1980 (Publication No. 3).
5. Corrosion of Magnesium at High Anodic Potentials, July, 1981 (Publication No. 5).

INDEX OF PUBLICATIONS

1. T. R. Beck, "Effect of Hydrodynamics on Pitting", Corrosion, 33, 9 (1977).
2. R. Alkire, D. Ernsberger, and T. R. Beck, "Occurrence of Salt Films During Repassivation of Newly Generated Metal Surfaces", J. Electrochem. Soc., 125, 1382 (1978).
3. T. R. Beck and R. D. Alkire, "Occurrence of Salt Films During Initiation and Growth of Corrosion Pits", J. Electrochem. Soc., 126, 1662 (1979).
4. T. R. Beck and S. G. Chan, "Experimental Observations and Analysis of Hydrodynamic Effects on Growth of Small Pits", Corrosion, (accepted for publication).
5. T. R. Beck and S. G. Chan, "Corrosion of Magnesium at High Anodic Potentials", to be submitted to J. Electrochem. Soc.; abbreviated version submitted to H. H. Uhlig 75th Birthday Symposium Volume, The Electrochemical Society, Fall Meeting, 1981.
6. T. R. Beck, Formation of Salt Films During Passivation of Iron", to be submitted to J. Electrochem. Soc.
7. T. R. Beck and S. G. Chan, "Corrosion of Aluminum at High Anode Potentials", to be submitted to J. Electrochem. Soc.
8. T. R. Beck, "Pitting of Titanium, III Electrical Properties of Salt Film", to be submitted to J. Electrochem. Soc.

EXTENDED ABSTRACTS

1. R. C. Alkire, D. W. Ernsberger and T. R. Beck, The Occurence of Salt Films During the Initial Stages of Corrosion, Ext. Abs. No. 93, The Electrochemical Society, Fall Meeting, Las Vegas, NV, October 17-22, 1976.

2. T. R. Beck, Pitting of Titanium, III Electrical Properties of Salt Film, Ext. Abs. No. 64, The Electrochemical Society, Spring Meeting, Seattle, WA, May 21-26, 1978.

3. T. R. Beck, Formation of Salt Films During the Passivation of Iron, Ext. Abs. No. 128, The Electrochemical Society, Fall Meeting, Pittsburgh, PA, October 15-20, 1978.

4. T. R. Beck and S. G. Chan, Experimental Observation and Analysis of Hydrodynamic Effects on Growth of Small Pits, Ext. Abs. No. 239, The Electrochemical Society, Fall Meeting, Los Angeles, CA, October 14-19, 1979.

5. T. R. Beck, Corrosion of Aluminum and Magnesium in some Organic Solvents, Ext. Abs. No. 159, The Electrochemical Society, Fall Meeting, Hollywood, FL, October 5-10, 1980.

6. T. R. Beck and S. G. Chan, Corrosion of Magnesium at High Anodic Potentials, Ext. Abs. No. , The Electrochemical Society, Fall Meeting, Denver, CO, October 11-16, 1981.